

## Terahertz Vibrometer that Senses Sub-micron Vibrations Behind Barriers

Jerry C. Chen and Sumanth Kaushik

M.I.T. Lincoln Laboratory

244 Wood St, Lexington, MA 02420

jcchen@ll.mit.edu, skaushik@ll.mit.edu

### INTRODUCTION

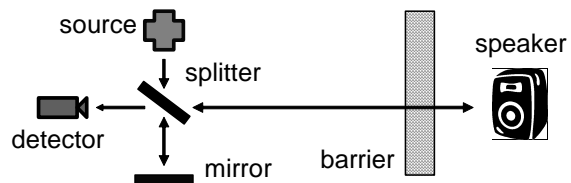
The far infrared or terahertz regime is one of the least understood areas of the optical spectrum. Recently, the far infrared has been an active area of research<sup>1-2</sup>, and has been proposed for various homeland security applications<sup>3</sup>. Because terahertz is relatively eye safe and can penetrate visibly opaque barriers like plastic, bags, cardboard and clothing, it has been proposed for imaging and identifying explosives and drugs<sup>4</sup>. In addition, far infrared or terahertz sensors have been able to pinpointing knives in envelopes and powders in plastic boxes<sup>5</sup>. For commercial, non-military scenarios, terahertz has been used to map veins of leaves<sup>6</sup>, calculate radar crosssections<sup>7</sup>, characterize burns in tissues<sup>8</sup>, find voids in foam<sup>9</sup>, etc. From spectroscopic lines and transitions, vibrations of molecular species have been inferred<sup>10</sup>.

But to our knowledge, terahertz has never been applied to measure vibrations of macroscopic objects. This non-contact sensing of vibrations could be useful for studying motors, audio speakers, membranes, fans, etc that are covered or concealed behind optically opaque materials such as plastic, cloth, paper, etc.

Here we describe the first vibration sensor based on far infrared or terahertz light. This novel sensor uses commercial components, runs at room temperature and needs minimal processing. This paper will detail the design principles and then present some experimental data.

### THEORY

Our terahertz sensor can be constructed from a Mach Zehnder or a Michelson interferometer. Aligning a Michelson is easier. Michelson's have been used in terahertz OCT (optical coherence tomography) with broadband or low coherence sources<sup>11-2</sup>. However, in this case, we prefer narrow band or high coherence sources to ease matching the interferometer's arm lengths. The terahertz radiation is collimated onto a beam splitter (figure 1). Part of the energy goes to the reference arm where it is retro-reflected by a mirror. In the device under test (DUT) arm, the rest of the energy passes through a barrier to the DUT, where it is reflected back through the barrier. Then energy from both arms combine coherently at the detector. Vibrations induce phase changes, which the interferometer converts to amplitude variations. This sensor is based on the well known



homodyne configuration. Heterodyne would have given better performance but it is not trivial to frequency shift in the far infrared.

Figure 1: Block diagram of experimental setup: terahertz sensor, barrier, and audio speaker.

---

This work is sponsored by the Department of the Air Force under AF Contract #FA8721-05C-0002. Opinions, interpretations, recommendations and conclusions are those of the authors and are not necessarily endorsed by the United States Government

The received power can be expressed as

$$P_{RX} = PRT(1 + L^2 + 2L \cos(\phi_1 - \phi_2)),$$

where P is transmit power, R is the fractional power reflected, T is fractional power transmitted through beam splitter, L is the fractional power transmitted through barrier during one pass, and  $\phi_1 - \phi_2$  is the phase difference between the interferometer arms. In turn, this phase difference is

$$\phi_1 - \phi_2 = \phi_{DC} + 2k \sum_i D_i \sin(\omega_i t),$$

where D is the vibration's maximum displacement,  $\omega$  is the vibration's frequency, k is the wave vector, and  $\phi_{DC}$  is the DC phase difference. In general each frequency component can be expressed in terms of Bessel functions. If  $\phi_{DC}/\pi$  is a half integer, the received power simplifies to

$$P_{RX} = PRT(1 + L^2 \pm 4Lk \sum_i D_i \sin(\omega_i t) + \dots)$$

for small displacements. The sign is minus for  $\phi_{DC}/\pi = 2m + \frac{1}{2}$  and the sign is plus for  $\phi_{DC}/\pi = 2m - \frac{1}{2}$ , where m is an integer.

## EXPERIMENT

To demonstrate the feasibility of this sensor concept, we built a table top version. The narrowband terahertz source could be a quantum cascade laser or a CO<sub>2</sub> laser pumped gas cell. We use a Microtech backward wave oscillator with an ov-80 tube, which emits about 3 mW at 615 GHz or 488  $\mu\text{m}$ . Broadened by voltage modulation, its linewidth is 60 MHz. A 60 mm focal length polyethylene lens collimates the beam. The beam splitter is a 25  $\mu\text{m}$  thick Kapton film whose estimated transmission is 70%. A spectrally flatter alternative is a thin, high resistivity silicon window, but we were not able to obtain one at the time. The reference mirror is a flat aluminum surface mounted on a XYZ stage. The detector is a Golay cell on loan from Microtech Instruments. The detector's output was sent to a RF spectrum analyzer, a HP 3562A, where the spectrum was averaged 10 times with a single integration time of 1.6 seconds. The Golay's responsivity drops rapidly with modulation frequency; the 3 dB point is 45 Hz. We wish to sense vibrational frequencies much higher than 45 Hz. So, a computer divides the measured voltage at each frequency point by the Golay's responsivity at that frequency. This

“pre-emphasis” extends the Golay's useful electrical bandwidth. As an alternative, we could have used a pyroelectric detector but their noise equivalent powers are worse. Also, certain bolometers enjoy higher bandwidths and lower noises but need liquid helium cooling. The device under test (DUT) is a small aluminum mirror mounted on a speaker. This speaker is driven by 40, 100 and 130 Hertz tones. Both the DUT and reference mirrors were 2.5 inches from beam splitter. The first barrier was a cardboard box, whose transmission L is 0.33. We moved the reference mirror so the Michelson is biased near the half power point where it is most linear. If the source or tested device were moving, a servo loop would be needed to keep the mirror at a stable bias point.

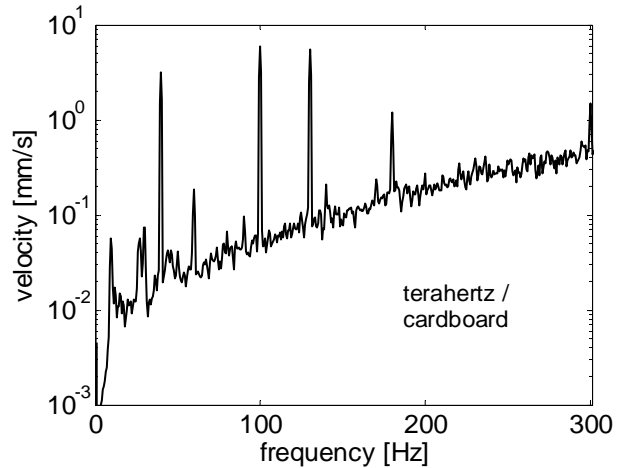


Fig. 2. Peak velocity of audio speaker versus vibration frequency, as measured by our 488  $\mu\text{m}$  sensor through a cardboard barrier.

Using our terahertz sensor, we plot the maximum velocity  $\omega D$  versus vibration frequency  $\omega/2\pi$  in figure 2. This 488  $\mu\text{m}$  vibrometer can clearly resolve the speaker tones at 40, 100 and 130 Hz and measures their peak velocities as 3.2, 6.0 and 5.5 mm/s respectively. Velocities are calibrated by maximizing the DC component of  $P_{RX}$  as the DC phase bias is varied. Specifically, if there is no barrier, the maximum value of  $P_{RX}$  gives 4 PRT. L was measured independently, but can be calculated by comparing the maximum  $P_{RX}$  with barrier to the  $P_{RX}$  without. The noise floor increases rapidly with frequency. Most of this

increase stems from the limited electrical bandwidth of the Golay. Some of the increase comes from multiplying the displacements  $D$  by frequency  $\omega$ . The velocity noise floor is about  $20 \mu\text{m/s}$  (or  $25 \mu\text{m/s}/\sqrt{\text{Hz}}$ ) for frequencies within the Golay electrical bandwidth of  $45 \text{ Hz}$ , and increases to  $60 \mu\text{m/s}$  (or  $75 \mu\text{m/s}/\sqrt{\text{Hz}}$ ) at  $100 \text{ Hz}$ . This corresponds to displacement noise floors of  $0.5 \mu\text{m}$  (or  $0.63 \mu\text{m/s}/\sqrt{\text{Hz}}$ ) at  $40 \text{ Hz}$  and  $0.6 \mu\text{m}$  (or  $0.75 \mu\text{m/s}/\sqrt{\text{Hz}}$ ) at  $100 \text{ Hz}$ . The Golay cell suffers from some electrical line noise at  $60$  and  $180 \text{ Hz}$ . Power supply filtering should be able to mitigate these spikes. We believe the ultimate noise floor is detector limited and would be lower with a liquid helium bolometer.

To validate our sensor's performance, we measure the same speaker with a HeNe based sensor, namely Polytec's PDV100. Since  $632 \text{ nm}$  can not penetrate cardboard, we removed the barrier so the HeNe has direct line of sight to the speaker. Output from the PDV100 is sent to the HP 3562A where the spectrum is calculated and averaged. This vibrational spectrum is plotted in figure 3. The

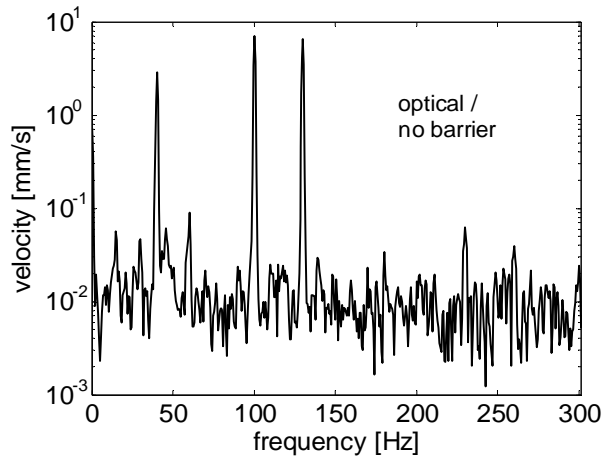


Fig. 3. Peak velocity of audio speaker versus vibration frequency, as measured by a HeNe-based vibrometer. There is no barrier.

Polytec measures the  $40$ ,  $100$ , and  $130 \text{ Hz}$  vibrations as  $2.9$ ,  $7.1$  and  $6.5 \text{ mm/s}$  respectively, which is consistent with the terahertz sensor. The noise floor from  $0$  to  $300 \text{ Hz}$  is about  $20 \mu\text{m/s}$  (or  $25 \mu\text{m/s}/\sqrt{\text{Hz}}$ ). The HeNe sensor also sees a  $60$  and  $180 \text{ Hz}$  noise spikes so the speaker polluted by the audio amplifier may be vibrating at  $60 \text{ Hz}$ . Both sensors see a  $15$  and  $30 \text{ Hz}$  vibration so that may be real as well. The small spikes at  $140$ ,  $170$ , and  $230 \text{ Hz}$  reflect second order intermodulation distortion of the speaker and its audio amplifier. The terahertz sensor has these speaker intermods, as well as additional second order intermods and harmonics from biasing the interferometer slightly off quadrature. Overall, the two sensors have good spectral agreement. However, the terahertz sensor does have the advantage of being able to measure behind cardboard.

We found that the  $488 \mu\text{m}$  beam was able to transmit through other normally opaque barriers, too. We used a white cotton T shirt, a black wool vest, and a blue plastic recycling bin. The fractional power transmitted in a single pass through these barriers in the far infrared were  $L = 0.52$ ,  $0.39$ , and  $0.81$  respectively. In those experiments we drove the speaker with only a single sine wave at  $100 \text{ Hz}$ . The terahertz sensor was able to see that  $100 \text{ Hz}$  tone with good fidelity. Figure 4 plots the vibration's amplitude  $D$  versus vibration frequency  $\omega/2\pi$ , for the case of the wool vest. At  $100 \text{ Hz}$ , the amplitude is  $14 \text{ mm}$  and the noise floor is about  $40 \text{ nm}$  (or  $51 \text{ nm/s}/\sqrt{\text{Hz}}$ ). As in figure 2 there are spurious tones below  $50 \text{ Hz}$  and electrical line noise at  $60$  and  $180 \text{ Hz}$ . Unlike figure 2, there is a new vibration at  $200 \text{ Hz}$ . This tone is real, not a measurement artifact, because the HeNe based vibrometer also see a  $200 \text{ Hz}$  tone.

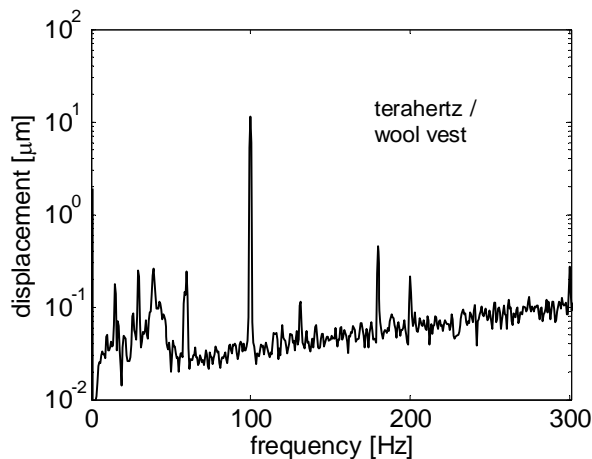


Fig. 4. Amplitude of audio speaker versus vibration frequency, as measured by our 488  $\mu\text{m}$  sensor through a wool vest.

## CONCLUSION

A novel 488  $\mu\text{m}$  (or 0.6 terahertz) sensor based on a Michelson interferometer has been modeled and built. Despite various optically opaque barriers, audio speaker velocities of 3 to 6 mm/s have been measured at 40 Hz with a noise floor of 20  $\mu\text{m/s}$  (or  $25 \mu\text{m/s}/\sqrt{\text{Hz}}$  in velocity or 0.1  $\mu\text{m}$  in displacement). Comparison with a commercial HeNe based vibrometer shows good agreement.

## ACKNOWLEDGMENT

We gratefully acknowledge Vladimir Kozlov of Microtech Instruments for loaning the Golay cell.

## REFERENCES

- <sup>1</sup> P. H. Siegel, "Terahertz technology," *IEEE Trans. Microw. Theory Tech.* **50**, 910-28 (2002).
- <sup>2</sup> S. P. Mickan and X.-C. Zhang, "T-Ray sensing and imaging" in *Terahertz Sensing Technology 1*, D. L. Woolward, W. R. Loerop, and M. S. Shur, eds. Singapore: World Scientific, 251-326 (2003).
- <sup>3</sup> W. R. Tribe, D. A. Newnham, P. F. Taday, and M. C. Kemp, "Hidden object detection: security applications of terahertz technology," in *Proc. of SPIE* **5354**, 168-76 (2004).
- <sup>4</sup> J. F. Federic, B. Schulkin, F. Huang, D. Gary, R. Barat, F. Oliveira and D. Zimdars, "THz imaging and sensing for security applications—explosives,

weapons and drugs," *Semicond. Sci. Technol.* **20**, S266-80 (2005).

<sup>5</sup> M. Hermann, R. Fukasawa, O. Morkawa, "Terahertz imaging" in *Terahertz Optoelectronics*, K. Sakai, ed. Berlin: Springer-Verlag, 331-81 (2005).

<sup>6</sup> B. B. Hu and M. C. Nuss, "Imaging with terahertz waves," *Optics Lett.* **20**, 1716-8 (1995).

<sup>7</sup> R. A. Cheville and D. Grischkowsky, "Time-domain terahertz impulse ranging studies," *Appl. Phys. Lett.* **67**, 1960-2 (1995).

<sup>8</sup> D. M. Mittleman, R. H. Jacobsen and M. C. Nuss, "T-ray imaging," *IEEE J. Sel. Topics Quantum Electron.* **2**, 679-92 (1996).

<sup>9</sup> H. Zhong, J. Xu, X. Xie, T. Yuan, R. Rieghtler, E. Madaras, X.-C. Zhang, "Nondestructive defect identification with terahertz time-of-flight tomography," *IEEE Sensors J.* **5**, 203-8 (2005).

<sup>10</sup> F. C. De Lucia, "Spectroscopy in the terahertz spectral region" in *Sensing with Terahertz radiation*, D. Mittleman, ed. Berlin: Springer-Verlag, 39-115 (2003).

<sup>11</sup> L. Johnson, T. D. Dorney, and D. M. Mittleman, "Interferometric Imaging with Terahertz Pulses," *IEEE J. Sel. Topics Quantum Electron.* **7**, 592-8 (2001).

<sup>12</sup> S. Krishnamurthy, M. T. Reiten, S. A. Harmon, and R. A. Cheville, "Characterization of thin polymer films using terahertz time-domain interferometry," *Appl. Phys. Lett.* **79**, 875-7 (2001).